PHILIPPINE ENGINEERING JOURNAL
PEJ 2006; **Vol. 27 No. 1**:29–42

Development of an Alternative Diagnostic Tool for Rupture Risk Assessment of Abdominal Aortic Aneurysms Using Finite Element Simulation

Louis Angelo M. Danao*and Andre S. Publico

Department of Mechanical Engineering
University of the Philippines Diliman
Quezon City 1101 PHILIPPINES

ABSTRACT

Abdominal aortic aneurysm (AAA) rupture is the 12th leading cause of death in the United States with a rank comparable to HIV/AIDS with deaths exceeding 12,000 a year. These deaths are preventable with early detection and elective repair. The current criterion for elective repair is an aneurysm with maximum diameter of 5.5 cm. But almost 25% of ruptures are less than or equal to 5 cm making the criterion an unreliable predictor of rupture. From a biomechanical perspective, the best indicator of rupture is wall stress when the mechanical stress induced exceeds the tensile strength of the tissue. One clinical case of AAA was the subject of this study. A published hyperelastic strain energy function was used as the material model for the AAA wall. Data from spiral computed tomography (CT) scans were used as a means of reconstructing the 3D geometry of the AAA. Using finite element method, the stress distribution on the aortic wall under systolic pressure was determined and studied. Wall stress was complexly distributed on the surface of the AAA, with distinct regions of high and low stress. Peak wall stress was found to be 0.55 MPa, located at the anterior portion of the AAA. A series of simulations were done to compute for the maximum wall stress in the AAA at increasing internal pressure and varying wall thickness. A map with von Mises stress (0.65 MPa) failure line indicating the failure zone plotted on pressure versus thickness charts is developed from the recorded maximum stresses. This is the proposed alternative tool to the single critical diameter criterion. This plot will be specific to a family of AAAs with maximum diameters falling within a particular range.
Keywords: abdominal aortic aneurysm, finite element, alternative diagnostic tool

1. INTRODUCTION

Abdominal aortic aneurysm (AAA) rupture is one of the leading causes of death in the United States with a rank comparable to HIV/AIDS with deaths exceeding 12,000 a year for both sexes over 65 years of age and 14,000 a year across all ages [7]. Risk factors include persons with ages greater than 55 years, history of smoking, high blood pressure, presence of any heart disease, and history in the family of AAA [25].

*Correspondence to: Department of Mechanical Engineering, University of the Philippines Diliman, Quezon City 1101 PHILIPPINES. email:louisdanao@up.edu.ph

Received May 23, 2007
Revised July 26, 2007
Accepted November 6, 2007

When AAA ruptures, 50% of the patients do not make it to the hospital alive while more than 40% die after emergency repair [38]. These deaths are preventable with early detection and elective repair. The current criterion for elective repair is an aneurysm diameter that is greater than 5.5 cm [24], when the risk of rupture is greater than the risk of surgery. But clinical cases have shown that rupture also occurs even when the aneurysm diameter is less than 5.5 cm.

Medical intervention by way of a graft inserted into the aneurysmal portion to prevent further ballooning also has risks with mortality rates at about 4-5% [16]. On top of that, the cost of surgery is restrictive. As such, precise determination of rupture risk is essential to give the required justification for surgery. Hence, a tool must be developed to provide the necessary information that will help in deciding if rupture is imminent or not.

2. METHODOLOGY

One patient at the Medical City Hospital in Pasig City, Philippines was the subject in this study. Spiral computed tomography (CT) data from this patient was used to create the 3D reconstruction of the infrarenal aorta. Abdominal CT scanning was performed with a Philips spiral CT scanner (model Brilliance 16). The slice thickness (collimation) was 5 mm with a helical pitch of 5 mm. After the raw spiral CT data were obtained, individual cross-sectional image slices were generated at 5 mm slice spacing along the infrarenal aorta.

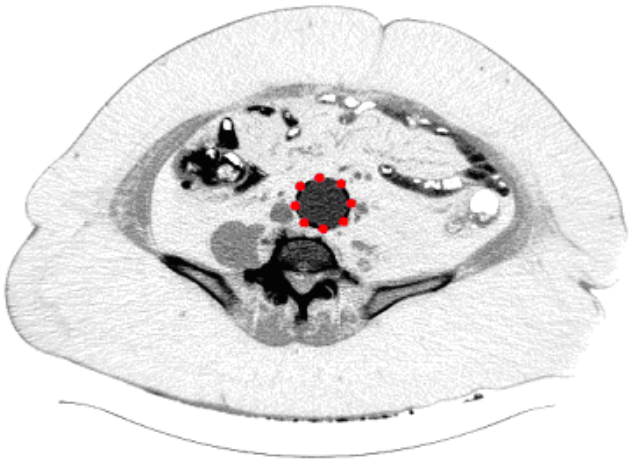

Figure 1. Digitizing the Boundary of the Aortic Wall using tpsDig2

Digital files containing the cross-sectional images were imported into the public domain image processing software tpsDig2 [36]. The boundary of the wall was identifiable while the

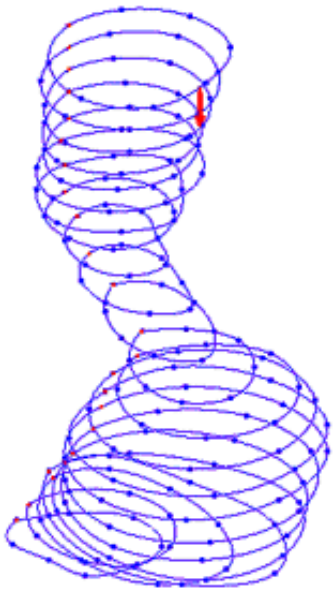

Figure 2. Cloud of Points for the Abdominal Aorta

thickness was not because of the low image resolution. The spatial coordinates of 8 points along the wall boundary were digitized for each cross section (Figure 1). Each 2D profile was outputted to a text file containing the x and y coordinates of each point. The coordinates of all the sections were combined into a single input file (ProEngineer Wildfire 2.0 input file, *.ibl) where the z-coordinate of each slice was subsequently added. From this, a point cloud was generated (Figure 2).

From the cloud of data points, a 3D surface (Figure 3) was created by importing the information into 3D modeling software ProEngineer Wildfire 2.0 [27]. The imported data was processed using the blend from file tool to create a shell model. A shell model was selected instead of a solid model because constant wall thickness will be used in the simulation. Irregularities (abrupt changes in contour) in the 3D model were refined by reducing the number of points per section. This is necessary to avoid singularities during finite element analysis. The final model was saved in the IGES format for importing to the finite element software.

In choosing the material model to be used, a published and widely used hyperelastic model was considered. Raghavan et al in 2000 proposed a constitutive material model for the AAA wall [29]. Their material model was assumed to be isotropic and hyperelastic. An approximate Mooney-Rivlin hyperelastic model was used for the material model as a substitute to the constitutive model proposed. This was done because a user-defined hyperelastic model was not available in the Academic license of the finite element software package Ansys 10.0. The

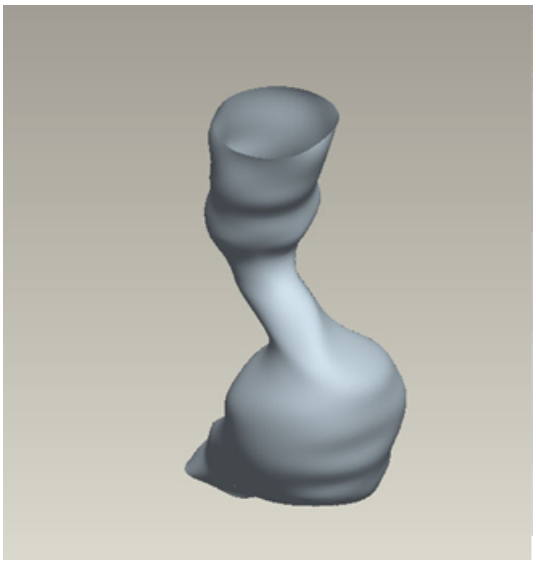

Figure 3. 3D Shell Model of the Abdominal Aorta

proposed constitutive model of Raghavan [29] was

$$W = \alpha \left(I_B - 3\right) + \beta \left(I_B - 3\right)^2 \tag{1}$$

where I_B is the first invariant of the Cauchy-Green tensor, and α and β are the mean of the material parameters determined from their experimental data.

The approximate Mooney-Rivlin hyperelastic model was derived using the 5 parameter option. Taking a look at the 5 parameter equation (Equation 2), we notice that there are a total of 6 constants that need to be defined. The Raghavan model [29] only has two material parameters present.

$$\begin{aligned} W &= c_{10}\left(\bar{I}_1 - 3\right) + c_{01}\left(\bar{I}_2 - 3\right) + c_{20}\left(\bar{I}_1 - 3\right)^2 \\ &\quad + c_{11}\left(\bar{I}_2 - 3\right)\left(\bar{I}_2 - 3\right) + c_{02}\left(\bar{I}_2 - 3\right)^2 + \frac{1}{d}\left(J - 1\right)^2 \end{aligned} \tag{2}$$

To get the approximate function, the following constants were adopted

$$\begin{aligned} c_{10} &= \alpha & c_{01} &= 0 \\ c_{20} &= \beta & c_{11} &= 0 \\ c_{02} &= 0 & d &= 0 \end{aligned}$$

where

$$\alpha = 17.4 \frac{N}{cm^2} \qquad \text{and}$$
$$\beta = 188.1 \frac{N}{cm^2}$$

All the terms containing the second invariant of the Cauchy-Green tensor are zeroed out. This is done to make the model consistent to the Raghavan hyperelastic model [29] where they assumed that the functional form of the strain energy density function is only in terms of the first invariant. There is no physical rationale to the assumption other than the mathematical model fits their experimental data very well. The material is assumed to be almost incompressible. This explains why the term containing the Jacobian will zero out because J is equal to one. To implement this in Ansys 10.0, the parameter d can be assigned the value of zero to zero out the last term.

The output file IGES was imported to finite element software ANSYS 10.0 and was assigned boundary conditions. Both the top and bottom sections of the model were constrained to move along the longitudinal direction (y-axis). One node at the bottom section was constrained in all displacement directions to prevent excessive deformation errors. An initial internal systolic pressure of 0.0160 MPa which is equivalent to 120 mm Hg was applied to the inner surface of the wall. Further simulations were made using higher systolic pressures.

Element definition proceeded with choosing a 4-noded shell element, SHELL181, with six degrees of freedom at each node: translations in the x, y, and z directions, and rotations about the x, y, and z-axes. SHELL181 is capable of bending as well as membrane effects and is well-suited for linear, large rotation, and/or large strain nonlinear applications. Assumed initial thickness of the shell was 1.5 mm. Further simulations were made using higher thickness values. Change in shell thickness is accounted for in nonlinear analyses. In the element domain, both full and reduced integration schemes are supported. Full integration was selected for the simulations. SHELL181 accounts for follower effects of distributed pressures.

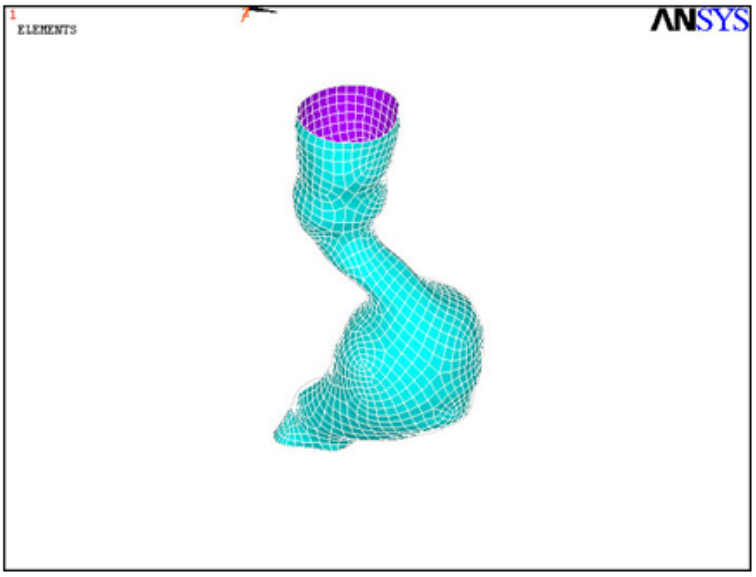

Figure 4. Meshed 3D Model

The whole model was meshed using the software's built-in meshing algorithm "SMART SIZING" with a setting of "6" (Figure 4). Quad-shaped elements were chosen to give better

accuracy in the results. Static, large displacement analysis was performed with a minimum of 100 load sub steps implemented. Nodal contour plots of the von Mises stress was used to evaluate the stress state of the model.

3. RESULTS

The maximum diameter of the AAA was found to be 5.1 cm using an in-house program. The von Mises stress distribution on the AAA of the study subject was plotted and observed. Stress is a tensor quantity with nine components. The von Mises stress is a stress index especially suited for failure analysis and is a combination of these nine components. Studying the von Mises stress, rather than each component of stress, allows for meaningful interpretation of the results. The 3D distribution of von Mises stress on the aortic wall is shown in Figure 5. It can be observed that the value of the peak wall stress is 0.55245 MPa. The location is not visible in the plot as it was determined that the location of the peak wall stress was located inside the AAA, as shown in Figure 6. This was expected because the element used in the simulation (SHELL181) was capable of computing for bending as well as membrane stresses. This tells us that the stress through the thickness of the wall is not single-valued but also varying.

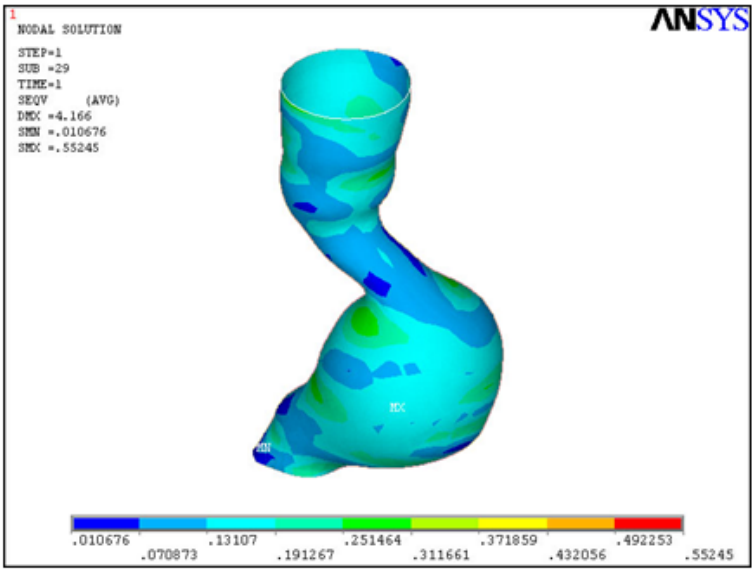

Figure 5. Von Mises Stress Plot of the Aorta

The corresponding von Mises strains were also investigated and the distribution plot is shown in Figure 7. It can be observed that the maximum strain is located in the same vicinity as the maximum stress. The maximum strain computed was 0.17863.

Table I shows the maximum values of the principal stresses and strains and the von Mises stress and strain and their locations (node numbers). The location of maximum von Mises strain corresponds to the location of maximum von Mises stress.

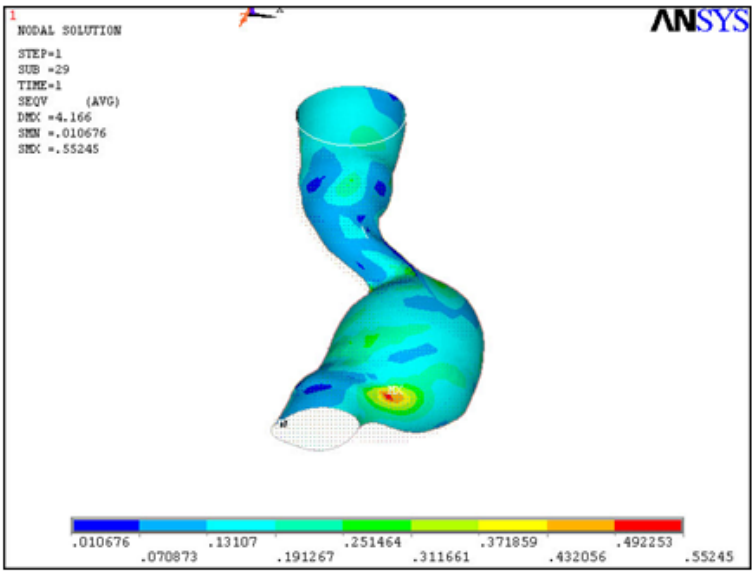

Figure 6. Sectional View of Aorta Showing Maximum von Mises Stress Location

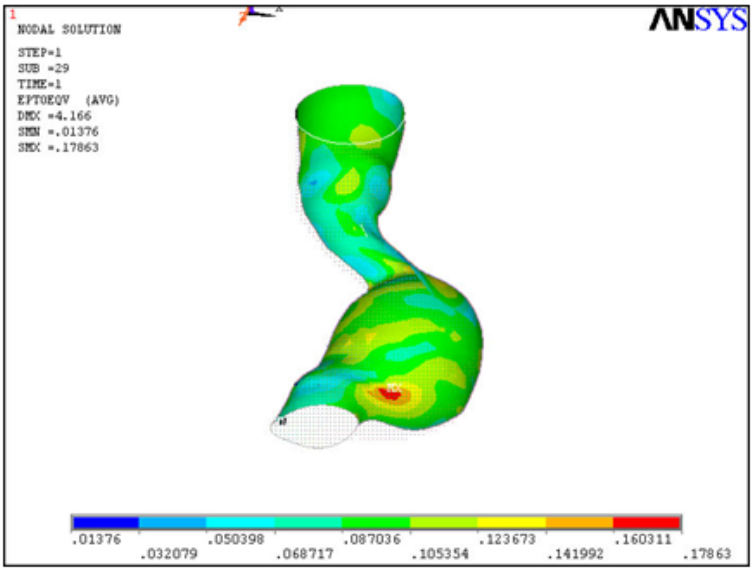

Figure 7. Von Mises Strain Plot of the Aorta

4. DEVELOPMENT OF ALTERNATIVE TOOL

From a basic mechanics perspective, problems involving structural stress analysis require a minimum set of parameters for the problem to be solvable. These are the physical dimensions,

MAXIMUM VALUES OF STRESS					
	S1	S2	S3	SINT	SEQV
NODE	2108	2108	169	2108	2108
VALUE	0.65313	0.28605	0.30672 E-01	0.63536	0.55245

MAXIMUM VALUES OF STRAIN					
	EPTO1	EPTO2	EPTO3	EPTOINT	EPTOEQV
NODE	733	1431	810	2108	2108
VALUE	0.15026	0.59889 E-01	-0.72934 E-02	0.29227	0.17863

Table I. Maximum Values of Stress and Strain

material properties, loading conditions, and boundary conditions. In the case of an AAA, the predominant physical dimension being considered is the maximum aortic diameter. This is very simplistic but nonetheless a significant consideration. To make the problem more realistic, more physical dimensions should be considered. If we simplify the AAA problem into a cylindrical shell, wall thickness is an indispensable parameter. It is proposed that the new diagnostic tool must include actual wall thickness as a critical factor. On top of taking into account the actual wall thickness of an AAA, actual loading conditions must also be a component of the diagnostic tool. Having said that, the obvious addition to the diagnostic tool is the systolic pressure. This, along with maximum diameter and wall thickness, will provide a tool that covers more ground than the current maximum diameter criterion.

Multiple simulations were done on the model aorta using varying values of wall thickness and systolic pressure. Starting at 1.5 mm wall thickness, the aorta was loaded to 5 levels of systolic pressure from a normal 120 mm Hg to hypertensive pressures of 160 mm Hg. Maximum von Mises stress was recorded for each simulation. The wall thickness was then increased by 0.1 mm and the loading procedure was repeated. A maximum wall thickness of 2.1 mm was used. A plot of the von Mises stress versus wall thickness is presented in Figure 8. It can be seen from the plot that as the systolic pressure is increased, computed maximum von Mises stresses also increased. Material failure [30] is predicted at higher internal pressures with lower wall thickness.

A similar plot (Figure 9) was made showing maximum von Mises values versus systolic pressure. As expected, maximum stresses increase with increasing internal pressure. Material failure is again predicted at higher internal pressures with lower wall thickness.

For both plots (Figures 8 & 9), simple quadratic curve fitting was done to predict values of systolic pressures and wall thicknesses that correspond to material failure of 0.65 MPa von Mises stress. The resulting values are then plotted and shown in Figure 10. A quadratic curve fit was done to get a trend line that will represent the boundary between material failure and non-failure of aortic wall. This is shown in Figure 11. At this point, this is considered as the initial stage for the development of the alternative diagnostic tool.

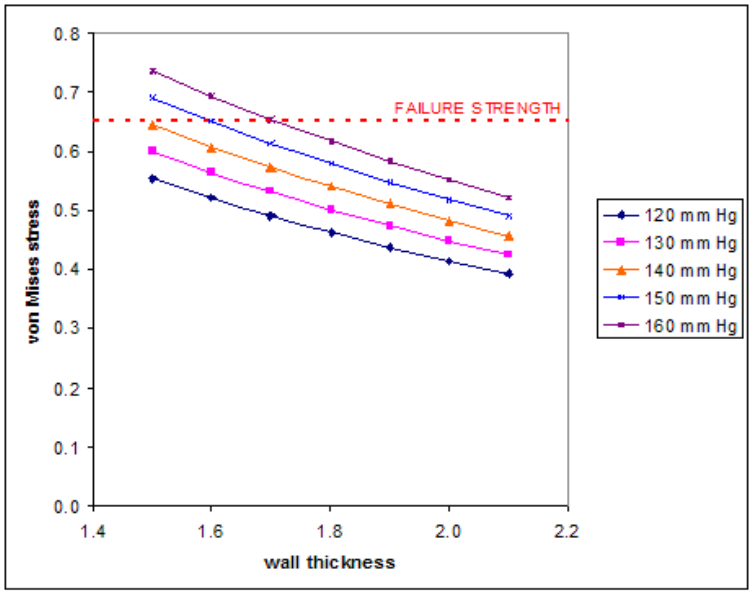

Figure 8. Von Mises Stress Versus Wall Thickness with Constant Systolic Pressure Lines

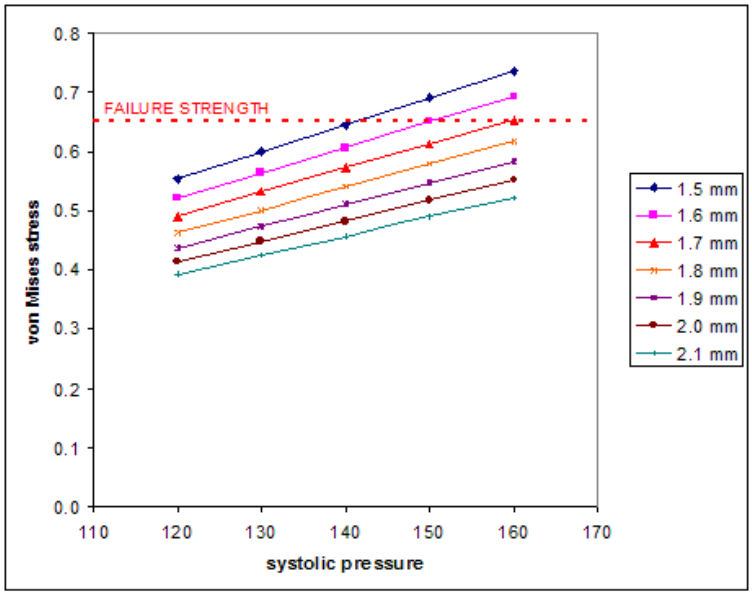

Figure 9. Von Mises Stress versus Systolic Pressure with Constant Wall Thickness Lines

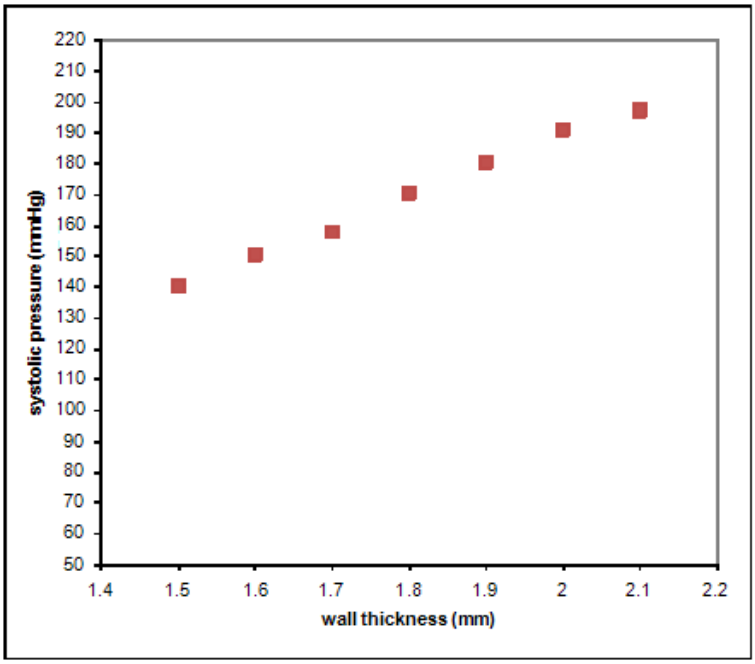

Figure 10. Predicted Plot of Systolic Pressure versus Wall Thickness at 0.65 MPa von Mises Stress

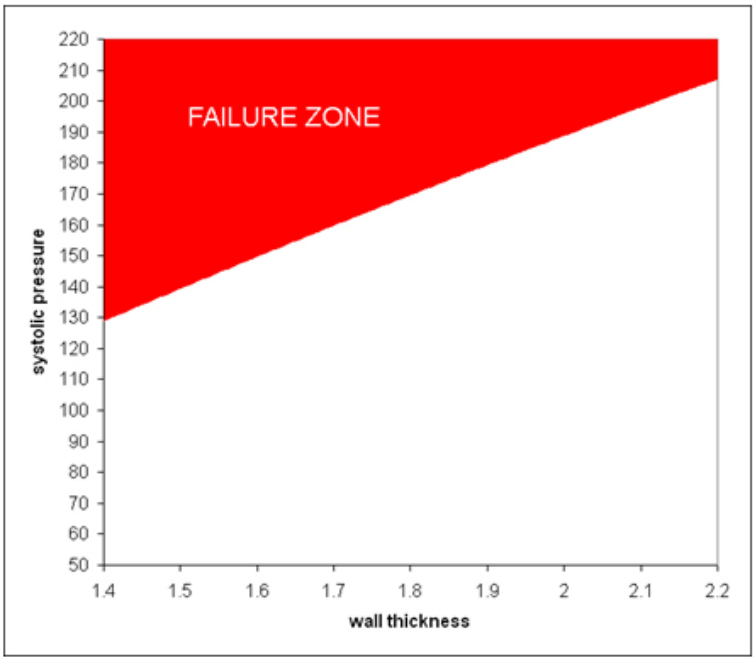

Figure 11. Proposed Form of the Alternative Diagnostic Tool

5. LIMITATIONS OF THE STUDY

Although much of the current research in the field of AAA mechanics deal with numerous considerations that play major roles in the actual behavior of the aneurysm, this study is limited to static, large displacement analysis of the aorta with no flow considerations. The available software that can be used is feature limited. Actual fluid flow effects cannot be tested in the Academic license of the finite element package. Also, the material model used is isotropic, hyperelastic in nature. A published orthotropic, hyperelastic material model is available for use but the academic license of the finite element software does not permit custom material models and no data is available for curve-fitting. Actual wall thicknesses were not considered because of the poor quality of the CT scans. Tests were made if solid elements could be used to allow non-uniform wall thickness in the simulation instead of shell elements but the license of the software limits the number of nodes to be used. Performing a full solid element simulation will require more nodes than what the software package allows.

6. CONCLUSIONS

The proposed diagnostic tool for rupture risk assessment of abdominal aortic aneurysms does not disregard the maximum aorta diameter as a critical parameter. In fact, the initial form of the tool is only specific to the clinical case used with a diameter of 5.1 cm. But in its early stages, the proposed diagnostic tool not only covers the existing criteria of maximum diameter, but it adds two other critical parameters for better assessment of rupture risk. Systolic pressure is a parameter that is easily obtained and measured. With the advances in medical imaging technology, wall thickness can be measured accurately with the use of cheap services such as ultrasound imaging.

A more comprehensive study must be done to consider the effects of varying maximum diameters. A population study must be conducted to give a better representation of maximum wall stresses at different aorta diameters. The final form of the proposed alternative diagnostic tool will be multiple plots of failure zones with systolic pressure and wall thickness as coordinate axes and each plot representing a family of aorta diameters (4 ˜ 5 cm, 5 ˜ 6 cm, 6 ˜ 7 cm, etc.).

7. RECOMMENDATIONS

Further research is proposed in light of the numerous limitations and assumptions made during the conduct of this study. It is desirable to perform simulations to multiple case studies to provide a better spread of the variability in geometries of the AAA specifically maximum diameter, actual wall thickness, and aorta asymmetry. Another important aspect that is recommended for future analysis is the anisotropy of the arterial wall. One major assumption in this study is that the AAA wall is isotropic in nature. A more up to date material model will provide an even more accurate pattern of stress distribution.

It should be realized that the 3D reconstruction of the AAA is actually a loaded state of the structure. The CT scans were taken from a live patient experiencing diastolic-systolic pressure cycles. Therefore, loading the AAA with a full systolic pressure is inaccurate and may be a

factor in the computation of high wall stress. To be able to come up with the unloaded state of the AAA will allow accurate simulation of the problem and better prediction of maximum stresses. An even further research can be done where actual pulsatile pressure cycles and shearing effects of fluid flow will be considered in the AAA to determine stress fluctuations during the cardiac cycle.

ACKNOWLEDGEMENTS

The author would like to acknowledge the invaluable assistance of Wang Wen Ping of CAD-IT Singapore, Alexander P. Paran, Ph.D. of the Department of Mechanical Engineering, and Mark Albert H. Zarco, Ph.D. of the Department of Engineering Sciences.

REFERENCES

1. Ailawadi G, Upchurch GR. The pathogenesis of abdominal aortic aneurysms. http://www.vascularweb.org. Date accessed: August 2005.
2. ANSYS Documentation for Release 10.0. Ansys, Inc., Houston, Pennsylvania. http://www.ansys.com.
3. ANSYS Multiphysics Release 10.0. ANSYS, Inc., Canonsburg, PA 15317, USA. http://www.ansys.com.
4. Basford JR. The Law of Laplace and its relevance to contemporary medicine and rehabilitation. Archives of Physical Medicine and Rehabilitation 2002; 83:1165-1170.
5. Bronzino JD (Editor-in-Chief). The Biomedical Engineering Handbook. Massachusetts: CRC Press, Inc., 1995. pp 254-303.
6. Carew TE, Vaishnav RN, Patel DJ. Compressibility of the arterial wall. Circulation Research 1968; 23:61-68.
7. Center for Disease Control. 20 Leading Causes of Death, United States. http://www.cdc.gov. Date Accessed: August 2005.
8. Chandrasekharaiah DS, Debnath L. Continuum mechanics. San Diego: Academic Press, Inc., 1994.
9. Chuong CJ, Fung YC. Compressibility and constitutive equation of arterial wall in radial compression. Journal of Biomechanics 1984; 17:35-40.
10. Di Martino E, Guadagni G, Corno C, Fumero A, Spirito R, Biglioli P, Redaelli A. Towards an index predicting rupture of abdominal aortic aneurysms. Proceedings of the 2001 Summer Bioengineering Conference, Utah; pp 821-822.
11. Fillinger MF, Marra SP, Raghavan ML, Kennedy FE. Prediction of rupture risk in abdominal aortic aneurysm during observation: Wall stress versus diameter. Journal of Vascular Surgery 2003; 37:724-732.
12. Fillinger MF, Raghavan ML, Marra SP, Cronenwett JL, Kennedy FE. In vivo analysis of mechanical wall stress and abdominal aortic aneurysm rupture risk. Journal of Vascular Surgery 2002; 36:589-597.
13. Guidant. What is an abdominal aortic aneurysm? http://www.guidant.com. Date accessed: August 2005.
14. Holzapfel GA, Eberlein R, Wriggers P, Weizscker HW. Large strain analysis of soft biological membranes: Formulation and finite element analysis. Computer Methods in Applied Mechanics and Engineering 1996; 132:45-61.
15. Hua J, Mower WR. Simple geometric characteristics fail to reliably predict abdominal aortic aneurysm wall stresses. Journal of Vascular Surgery 2001; 34:308-315.
16. Katz DA, Littenberg B, Cronenwett JL. Management of small abdominal aortic aneurysms: Early surgery to watchful waiting. Journal of the American Medical Association 1992; 268:2678-2686.
17. Kleinstreuer C, Li Z. Analysis and computer program for rupture-risk prediction of abdominal aortic aneurysms. Biomedical Engineering Online 2006; 5:19.
18. Lu J, Zhou X, Raghavan ML. Inverse elastostatic stress analylsis in pre-deformed biological structures: Demonstration using abdominal aortic aneurysms. Article in Press, Corrected Proof Journal of Biomechanics 2006.
19. Malvern LE. Introduction to the mechanics of a continuous medium. New Jersey: Prentice-Hall, Inc., 1969.
20. Maraon DP. Determination of locations of high wall stresses in an abdominal aortic aneurysm using computer simulation. Master's thesis. Mar 2005.
21. Mase GE, Mase GT. Continuum mechanics for engineers. Florida: CRC Press, Inc., 1992.
22. Mase GE. Schaum's outline series: Theory and problems of continuum mechanics. New York: McGraw-Hill, Inc., 1970.

23. MedlinePlus. Abdominal aortic aneurysm. http://www.nlm.nih.gov/medlineplus. Date accessed: August 2005.
24. Mortality results for randomised controlled trial of early elective surgery or ultrasonographic surveillance for small abdominal aortic aneurysms. The UK Small Aneurysm Trial Participants. Lancet 1998; 352:1649-1655.
25. National Aneurysm Alliance. What is AAA? http://www.screenaaa.org. Date accessed: August 2005.
26. Outten JT, Kruse KL, Freeman MB, Pacanowski JP, Ragsdale JW, Stevens SL, Goldman MH. Computational model of mechanical wall stress in abdominal aortic aneurysm one hour prior to rupture. Proceedings of the 2003 Summer Bioengineering Conference, Florida; pp 77-78.
27. ProEngineer Wildfire 2.0. Parametric Technology Corporation, Needham, MA 02494, USA. http://www.ptc.com.
28. Raghavan ML, Vorp DA, Federle MP, Makaroun MS, Webster MW. Wall stress distribution on three-dimensionally reconstructed models of human abdominal aortic aneurysm. Journal of Vascular Surgery 2000; 31:760-769.
29. Raghavan ML, Vorp DA. Toward a biomechanical tool to evaluate rupture potential of abdominal aortic aneurysm: Identification of a finite strain constitutive model and evaluation of its applicability. Journal of Biomechanics 2000; 33:475-482.
30. Raghavan ML, Webster MW, Vorp DA. Ex-vivo biomechanical behavior or abdominal aortic aneurysm: Assessment using a new mathematical model. Annals of Biomedical Engineering 1996; 24:573-582.
31. Sakalihasan N, Limet R, Defawe OD. Abdominal aortic aneurysm. The Lancet 2005; 365:1577-1589.
32. Society for Vascular Surgery. Abdominal aortic aneurysm. http://www.vascularweb.org. Date accessed: August 2005.
33. Stringfellow MM, Lawrence PF, Stringfellow RG. The influence of aorta-aneurysm geometry upon stress in the aneurysm wall. Journal of Surgical Research 1987; 42:425-433.
34. The Society of Thoracic Surgeons. Aortic Aneurysms. http://www.sts.org/sections/patientinformation/aneurysmsurgery/aorticaneurysms.
35. Thubrikar MJ, Al-Soudi J, Robicsek F. Wall stress studies of abdominal aortic aneurysm in a clinical model. Annals of Vascular Surgery 2001; 15:355-366.
36. tpsDig2. SUNY at Stony Brook Morphometrics. http://life.bio.sunysb.edu/morph.
37. Vande Geest JP, Sacks MS, Vorp DA. The effects of aneurysm on the biaxial mechanical behavior of human abdominal aorta. Journal of Biomechanics 2006; 39:1324-1334.
38. Venkatasubramaniam AK, Fagan MJ, Mehta T, Mylankal KJ, Ray B, Kuhan G, Chetter IC, McCollum PT. A comparative study of aortic wall stress using finite element analysis for ruptured and non-ruptured abdominal aortic aneurysms. European Journal of Vascular and Endovascular Surgery 2004; 28:168-176.
39. Vorp DA, Raghavan ML, Muluk SC, Makaroun MS, Steed DL, Shapiro R, et al. Wall strength and stiffness of aneurysmal and nonaneurysmal abdominal aorta. Annals of the New York Academy of Sciences 1996; 800:274-276.
40. Vorp DA, Raghavan ML, Webster MW. Mechanical wall stress in abdominal aortic aneurysm: Influence of diameter and asymmetry. Journal of Vascular Surgery 1998; 27:632-639.
41. Vorp DA, Rajagopal KR, Smolinski PJ, Borovetz HS. Identification of elastic properties of homogeneous, orthotropic vascular segments in distension. Journal of Biomechanics 1995; 28:501-512.
42. Wang DHJ, Makaroun MS, Webster MW, Vorp DA. Effect of intraluminal thrombus on wall stress in patient-specific models of abdominal aortic aneurysm. Journal of Vascular Surgery 2002; 36:598-604.
43. Wall tension and the law of laplace. http://www.lib.mcg.edu. Date accessed: May 2006.
44. Peterson LH, Jensen RE, Parnell J. Mechanical Properties of Arteries in Vivo. Circulation Research 1960; 8:622-639.

